JOURNAL OF GENERAL VIROLOGY

RESEARCH ARTICLE

Duffy *et al.*, *Journal of General Virology* 2018;99:135–147

DOI 10.1099/jgv.0.000978

Generation and characterization of a novel candidate gene therapy and vaccination vector based on human species D adenovirus type 56

Margaret R. Duffy,[1]†‡ Julio Alonso-Padilla,[2]†§ Lijo John,[3] Naresh Chandra,[3] Selina Khan,[4] Monika Z. Ballmann,[1] Agnieszka Lipiec,[1] Evert Heemskerk,[1] Jerome Custers,[4] Niklas Arnberg,[3] Menzo Havenga,[1] Andrew H. Baker[2,*]¶ and Angelique Lemckert[1,*]

Abstract

The vectorization of rare human adenovirus (HAdV) types will widen our knowledge of this family and their interaction with cells, tissues and organs. In this study we focus on HAdV-56, a member of human Ad species D, and create ease-of-use cloning systems to generate recombinant HAdV-56 vectors carrying foreign genes. We present *in vitro* transduction profiles for HAdV-56 in direct comparison to the most commonly used HAdV-5-based vector. *In vivo* characterizations demonstrate that when it is delivered intravenously (i.v.) HAdV-56 mainly targets the spleen and, to a lesser extent, the lungs, whilst largely bypassing liver transduction in mice. HAdV-56 triggered robust inflammatory and cellular immune responses, with higher induction of IFNγ, TNFα, IL5, IL6, IP10, MCP1 and MIG1 compared to HAdV-5 following i.v. administration. We also investigated its potential as a vaccine vector candidate by performing prime immunizations in mice with HAdV-56 encoding luciferase (HAdV-56-Luc). Direct comparisons were made to HAdV-26, a highly potent human vaccine vector currently in phase II clinical trials. HAdV-56-Luc induced luciferase 'antigen'-specific IFNγ-producing cells and anti-HAdV-56 neutralizing antibodies in Balb/c mice, demonstrating a near identical profile to that of HAdV-26. Taken together, the data presented provides further insight into human Ad receptor/co-receptor usage, and the first report on HAdV-56 vectors and their potential for gene therapy and vaccine applications.

INTRODUCTION

Decades of research into the family *Adenoviridae* has, for the most part, focused on human Ad type 5 (HAdV-5) as a prototype vector, with this providing the basis of our knowledge of Ad receptor/co-receptor usage, host interactions and immunogenicity. HAdV-5 has many desirable attributes, including ease of genetic manipulation, efficient production systems and the detailed characterization of its infection profiles. Despite the accumulation of years of clinical trial safety data, the evidence for therapeutic efficacy has been questionable, and this is in large part due to high levels of neutralizing antibodies against HAdV-5 in the general population capable of minimizing the active vector load, and/or poor or irregular expression and exposure of its cellular receptor [coxsackie and adenovirus receptor (CAR)] on cells and tissues of interest [1]. Given the large number of other Ad types available, the recent advances in DNA manipulation technologies and the convenience of CRISPR genome editing, there is significant interest in developing new viral vector strategies [2–6]. There is a need to find Ad types with low seroprevalence and alternative tropisms in place of HAdV-5, but without compromising on the ease of manufacture and vector yield [7, 8]. Thus investigation into the *in vitro* and *in vivo*

Received 15 August 2017; Accepted 2 November 2017

Author affiliations: [1]Batavia Biosciences BV, Leiden, The Netherlands; [2]Institute of Cardiovascular and Medical Sciences, College of Medicine, Veterinary and Life Sciences, University of Glasgow, Glasgow, UK; [3]Division of Virology, Department of Clinical Microbiology, Umeå University, Sweden; [4]Viral Vaccine Discovery and Early Development, Janssen Vaccines and Prevention BV, Leiden, The Netherlands.

***Correspondence:** Andrew H. Baker, Andy.Baker@ed.ac.uk; Angelique Lemckert, a.lemckert@bataviabiosciences.com

Keywords: adenovirus; HAdV-56; gene therapy; vaccine vector.

Abbreviations: CAR, coxsackie and adenovirus receptor; CL, clodronate liposomes; EKC, epidemic keratoconjunctivitis; HAdV, human adenovirus; HAdV-56, human adenovirus type 56; i.m., intramuscular; i.v., intravenous.

†These authors contributed equally to this work.

‡Present address: Department of Oncology, University of Oxford, Oxford, UK.

§Present address: Barcelona Institute for Global Health (ISGlobal), Centre for Research in International Health (CRESIB), Hospital Clinic de Barcelona -University of Barcelona, Barcelona, Spain.

¶Present address: Centre for Cardiovascular Sciences, Queen's Medical Research Institute, University of Edinburgh, Edinburgh, UK.

Four supplementary figures are available with the online version of this article.

biology of less prevalent virus types may advance the clinical use of Ad-based platforms.

HAdV species D (HAdV-D) is the largest of the seven human species, but very few of these Ads have been exploited as potential clinical tools. Most HAdVs belonging to other species use CD46, CAR or desmoglein 2 (DSG2) as high-affinity primary receptors for viral fibre proteins, and αv-integrins as co- or internalization receptors (referred to below solely as co-receptors) for viral penton base proteins [9]. Specific members of species D HAdV are reported to also use sialic acid-containing receptors and in particular a sialic acid-containing hexasaccharide that is identical to that of GD1a gangliosides [10–12]. In direct contrast to HAdV-5, the absence of pre-existing immunity to rare HAdV-D types [13] makes them good candidates for gene therapy or vaccine regimes. Here, we focus on a more recently discovered HAdV-D, Ad type 56 (HAdV-56), a member of the small subgroup of Ad causing the severe and highly contagious ocular infection known as epidemic keratoconjunctivitis (EKC). Whilst the complete genomic sequence for HAdV-56 is available (GenBank accession no. HM770721.2), important aspects of its biology and therapeutic applications remain unexplored. The arguments to investigate this virus stand on its predicted low seroprevalence, as HAdV-56 has a chimaeric hexon comprising rare HAdV-15 and HAdV-29 viruses with a fibre protein that is most similar to HAdV-9 [14]. Furthermore, the ability of HAdV-56 to cause potent infections with marked ocular tropism suggests that it may use non-classical receptors/co-receptors or possess interesting immune modulatory elements [14]. In the present study we generate novel E1/E3-deleted, replication-deficient reporter vectors based on HAdV-56 as tools to study its biology. These recombinant HAdV-56 (rHAdV-56) vectors are used to characterize the seroprevalence, receptor/co-receptor usage and tropism of their parental serotype, while we also provide valuable information on the potential of HAdV-56 as a vascular gene therapy and vaccine vector.

RESULTS

Generation of replication-deficient HAdV-56 vectors expressing reporter genes

We first generated HAdV-56 vectors expressing reporter genes to enable us to study the virus biology and its therapeutic applicability efficiently. To produce replication-incompetent reporter viruses, the E1 gene of HAdV-56 was replaced with luciferase, GFP or LacZ in a shuttle plasmid containing a multiple cloning site for the easy insertion of foreign genes. The E3 region was also deleted to increase transgene packaging capacity. To enhance the potential for viral propagation in a standard producer cell line, the HAdV-56 E4ORF6 region was exchanged with that of HAdV-5, as this strategy was previously reported to enhance the growth of recombinant Ad vectors in HAdV-5 E1-complementing HEK293 cells [15, 16]. A schematization of the cloning system and HAdV-56 vector (rHAdV-56.ΔE1.ΔE3.Ad5.E4ORF6) genome organization is shown in Fig. 1. At approximately 14 days post-co-transfection of HAdV-56-based plasmids, cytopathic effect (CPE) was observed and viral progeny were successfully propagated. The resulting vectors were verified by DNA sequencing and all were found to express their corresponding transgene efficiently, as assessed by luciferase assay, fluorescence microscopy and β-galactosidase staining of HAdV-56-Luc-, HAdV-56-GFP- and HAdV-56-LacZ-infected cells, respectively. All vectors were grown to high titres and good quality purified vector batches were produced by standard CsCl purification systems (see Fig. S1, available in the online version of this article for silver stain and Western blot analysis).

Manufacture of HAdV-56 vectors

During the preclinical development stage it is important to consider whether the vector of interest is amenable to manufacturing protocols and the rigorous quality controls required in cases of clinical translation. Even though manufacturing systems are developed for the HAdV-5-based vectors that are used as standard, such systems do not always work as well for other Ad vectors. In order to investigate whether the HAdV-56 vectors could also be produced and purified utilizing such manufacturing procedures, HEK293 suspension cells were infected with rHAdV-56 utilizing GMP-compliant and commercially available media (EX-CELL 293, AEM, CD293, CDM4-HEK293, SFM4-HEK293 and EX-CELL GTM-3) at cell densities of 1.5×10^6 cells ml^{-1}. All of the tested media showed comparable $\log_{10}$ $TCID_{50}$ ml^{-1} yields (8.39 to 9.54) (Fig. S1b). Traditionally, Ad vectors are purified using Mustang Q filters as the first capture step. Therefore we investigated whether Mustang Q filters are a suitable capture entity for rHAdV-56, and broadened the investigation by looking at alternative filters such as Poros HQ and Monolith QA. All of the tested entities worked well for the rHAdV-56 capture purification step, but our results indicate that Poros HQ has the best recovery and purity (Fig. S1c–e). Looking at these manufacturing parts, we conclude that rHAdV-56 can be produced to high titres and then purified to a high degree of purity in manufacturing settings, an essential criterion for the large-scale GMP production required for many clinical applications.

Characterization of HAdV-56 receptor/co-receptor usage

Unlike the well-studied Ad gene therapy or vaccination vectors (e.g. HAdV-5, HAdV-26 and HAdV-35), HAdV-56 belongs to a small group of Ad-Ds that have been reported to be causative agents of EKC, which is suggestive of alternative infection profiles and potentially different entry receptors/co-receptors. Being associated with ocular, respiratory and urinary tract disease [17–20], HAdV-56 infection of corneal cells has been documented [20], but studies investigating the transduction of other cell types and receptor/co-receptor usage are limited. Therefore the transduction capacity of the novel HAdV-56 vectors was assessed in the classical CAR-abundant lung adenocarcinoma A549 cells and CAR-low ovarian

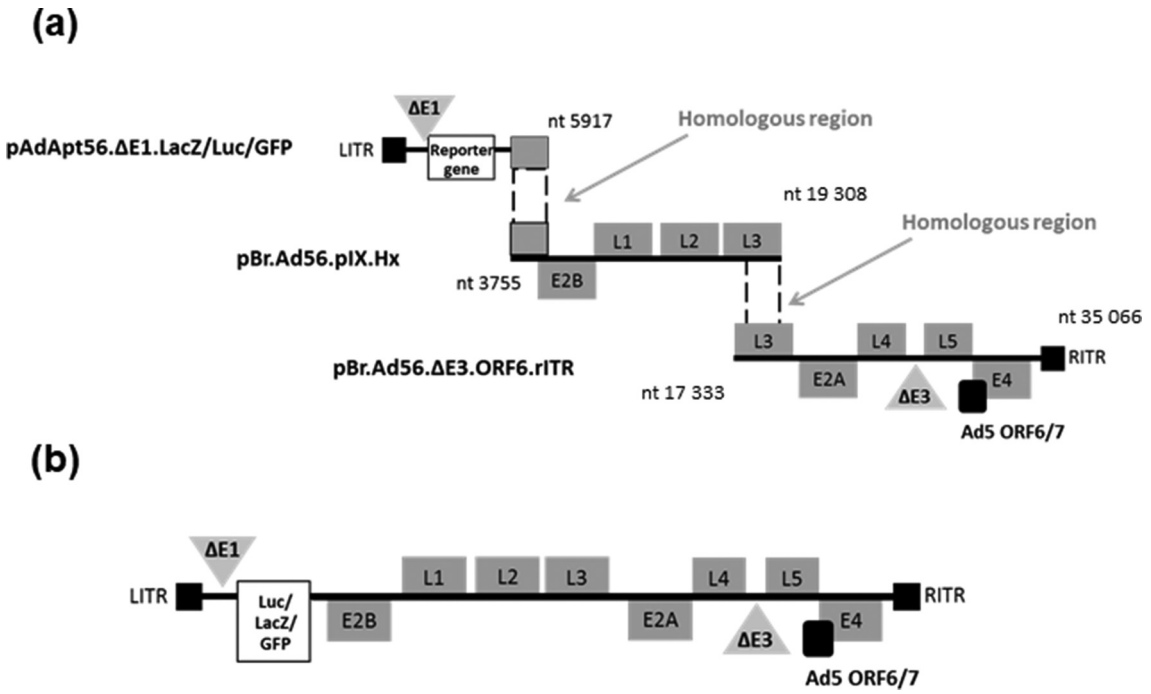

Fig. 1. HAdV-56 vector generation. (a) Schematic representation of the replication-deficient recombinant HAdV-56 vector construction strategy using a three-plasmid system (pAdApt56.ΔE1.Luc, LacZ or GFP, pBr.HAdV-56.pIX.Hx and pBr.HAdV-56.ΔE3.ORF6.rITR) and highlighting the regions involved in homologous recombination, the viral early (E) and late (L) genes. (b) Genome organization of the recombinant HAdV-56 vector (rHAdV-56.ΔE1.ΔE3.5ORF6) expressing luciferase, GFP or LacZ genes.

carcinoma SKOV3 cell line [Fig. 2(a, b), Fig. S2], and compared to HAdV-5. Luciferase activity upon the transduction of SKOV3 cells was very similar for both HAdV-56-Luc and HAdV-5-Luc, whilst HAdV-5-mediated transgene expression in A549 cells was significantly higher than that of HAdV-56 (Fig. 2a, b). The levels of HAdV-56 luciferase activity in both cell lines were very similar at all vector particles per cell (VP/cell) ratios tested (~1.0×10^7–2.2×10^8 RLU). Similar transduction experiments were performed in CHO-K1- and CHO-CAR-expressing cells. CAR receptor expression enhanced HAdV-5 transgene levels, whilst it had little impact on the overall levels of the HAdV-56 transduction of CHO cells (Fig. 2c, d). Taken together, these data indicate that whilst HAdV-5 avails of CAR-mediated entry, high levels of CAR expression do not boost HAdV-56 transduction.

Sialic acid-containing glycans have previously been demonstrated to be primary receptors for HAdV-D infection [12]. Here we examined the role of sialic acid in HAdV-56 binding and infection of human corneal epithelial cells using neuraminidase to knockdown sialic acid residues. Whilst blocking sialic acids did hinder HAdV-56 binding to the cell surface initially, overall infection levels after an incubation of 44 h were unaffected (Fig. 3a, b). Taken together, these data suggest that, unlike other HAdV-D viruses, HAdV-56 does not require sialic acids as a primary receptor for efficient infection.

Next, to examine the role of cellular integrins in HAdV-56 infection, we utilized CHO cells stably expressing a range of different human integrins, including $\alpha4\beta1$, $\alpha4\beta7$, αv, $\alpha2\beta1$, $\alpha3$, $\alpha5$, $\alpha6$, $\alpha7$, $\alpha8$ and $\alpha9$ subunits [21–27]. CHO-B2 (lacking expression of the $\alpha5$ subunit [28]) and CHO-K1 (expressing native $\alpha5$) cell lines were used as negative controls for these experiments. GFP-encoding HAdV-56 transduced CHO-$\alpha7$ cells at substantially higher levels (seven-fold greater) compared with the CHO control cells (Fig. 3c, d), whilst there was no increase in the transduction levels of HAdV-5 in these cells. This is the first example of an Ad utilizing integrin-$\alpha7$ as a potential entry receptor or co-receptor. The levels of HAdV-56 transgene expression were also significantly raised in αv integrin-expressing CHO cells. Taken together, these data indicate that integrin subunit $\alpha7$, and to a lesser extent subunit αv, can function as entry receptors or co-receptors for HAdV-56, thereby adding to our knowledge of the diverse Ad family.

Previous studies have shown that integrin subunit $\alpha7$ is expressed at high levels in muscle tissue, including skeletal and cardiac, as well as vascular, gastrointestinal and genitourinary smooth muscles [29, 30], suggesting that rHAdV-56 may be a candidate vector for vascular gene therapy or intramuscular delivery applications. To test this, primary human saphenous vein smooth muscle cells (HSVSMCs) and human saphenous vein endothelial cells (HSVECs) were isolated (n=3 individual patients), and the transduction

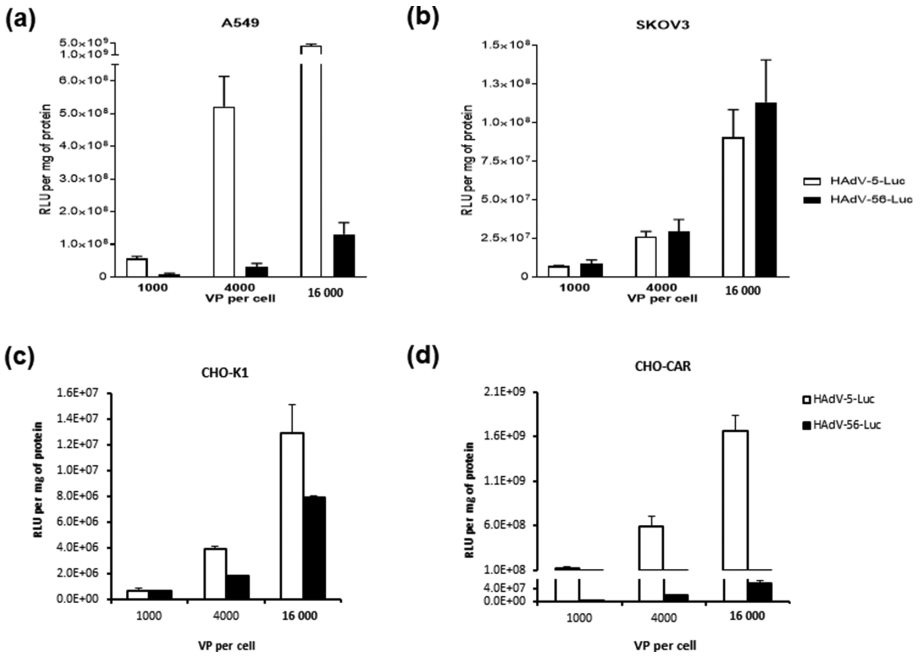

Fig. 2. HAdV-56 transduction *in vitro*. HAdV-56-Luc transduction assay on (a) A549, (b) SKOV3, (c) CHO-K1 and (d) CHO-CAR cells in comparison to HAdV-5-Luc.

ability of HAdV-56-Luc was evaluated using these cells. HAdV-56 mediated similar levels of luciferase transgene expression at all of the VP/cell ratios tested to HAdV-5-Luc (Fig. S3), indicating its potential for development as a vascular targeted vector.

HAdV-56 vector interactions with serum and coagulation factors

Whilst HAdV-5-based vectors mediate high levels of gene expression *in vitro*, they are severely compromised when it comes to intravenous (i.v.) administration *in vivo* due to an abundance of neutralizing antibodies and tropism-altering interactions with blood components [31, 32]. As i.v. delivery is the optimum and least invasive route for many clinical applications, developing Ad types with good blood stability is of significant interest.

We investigated the levels of pre-existing neutralizing antibodies against HAdV-56 using a panel of serum samples (n=103) taken from a cohort of healthy >50-year-old US citizens. Whilst 57 % of the serum samples exhibited high levels of neutralizing activity (effective at dilutions >1 : 200) against HAdV-5, less than half of these were inhibitory to HAdV-56, i.e. 28 % of serum samples neutralized HAdV-56 activity at dilutions >200 (Fig. 4a). Whilst HAdV-56 has higher seroprevalence than the rare species B HAdV-35 (only 11 % neutralized at 1 : 200 serum dilution), these data indicate that antibodies against HAdV-56 are at substantially lower levels in the general population than those against HAdV-5.

The binding of many Ad types to human coagulation blood factor X (FX) has a significant impact on virus transduction *in vitro* and is a major determinant of tropism *in vivo* following i.v. administration [31, 33, 34]. We investigated whether blood coagulation factors affect HAdV-56 transduction. Physiological concentrations of human factor VII (FVII), factor IX (FIX), factor X (FX) and protein C (PC) were incubated with cells prior to the addition of HAdV-56 or HAdV-5 vectors. Unlike HAdV-5, HAdV-56 luciferase reporter activity remained constant in A549 or SKOV3 cells regardless of the addition of FVII, FIX, FX or PC (Fig. 4b, c), thereby demonstrating that the transduction of HAdV-56 is not augmented by any of the blood coagulation factors tested.

Taken in combination, the lower seroprevalence and the lack of influence from coagulation factors, indicates the more favourable characteristics of HAdV-56 compared to HAdV-5 for systemic delivery.

HAdV-56 biodistribution following i.v. delivery *in vivo*

To characterize the HAdV-56 vectors following i.v. administration *in vivo*, we evaluated the biodistribution patterns of HAdV-56-Luc using a previously described mouse model [35, 36]. Vehicle (PBS) and HAdV-5-Luc-inoculated animals were included in this study as negative and positive control groups, respectively. Half of the animals were pretreated with clodronate liposomes (CL+) for macrophage depletion as they are known to play a major role in HAdV-5 liver sequestration, and the rest of the mice were

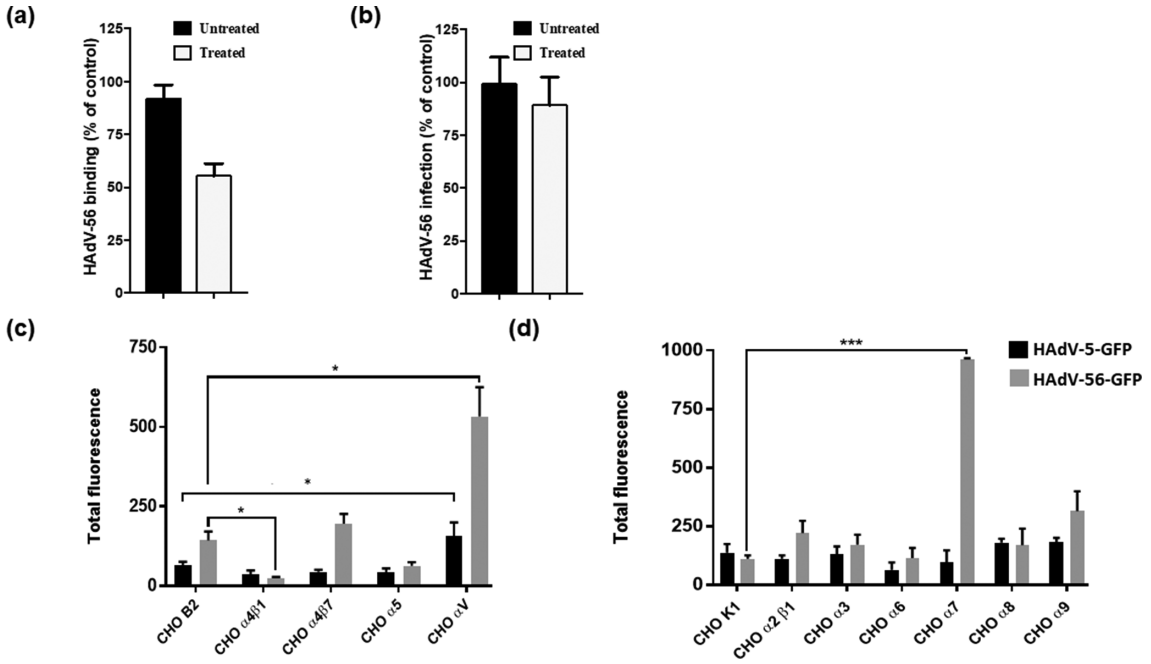

Fig. 3. HAdV-56 use of co-receptors. HAdV-56 binding to (a) and infection of (b) human corneal epithelial cells treated with and without 20 mU ml^{-1} neuraminidase. Susceptibility of integrin-expressing CHO cells to HAdV-56-GFP and HAdV-5-GFP transduction; (c) CHO-B2 and (d) CHO K1 cells were used as negative control cell lines. The results are presented as mean±SEM. Statistical significance was determined by *t*-test and the Bonferroni post hoc test. Asterisks indicate the level of significance. **P* <0.05, ****P* <0.005 versus control cell lines.

untreated (CL−, intact macrophages). Two days after vector administration the animals were IVIS imaged and then sacrificed, and several organs were collected and processed for Ad DNA quantification and luciferase activity measurements (Fig. 5a–c). On average, HAdV-5 and HAdV-56 mediated luciferase expression and the vector genome copies were 10-fold higher in CL+-treated animals compared to the CL− groups. As expected, HAdV-5-derived genomes and transgene expression were focused in the liver and spleen. In both CL−- and CL+-treated animals, HAdV-56 DNA and luciferase transgene expression were most abundant in the spleen, with low levels observed in the lungs and pancreas, and liver transduction was bypassed (Fig. 5a–c).

Elevation of the liver enzymes aspartate aminotransferase (AST) and alanine aminotransferase (ALT) can be used as an indicator of liver damage post-injection of Ad vectors. In macrophage-depleted animals (CL+) injected with HAdV-5-Luc, AST levels were significantly increased with respect to clodronate-treated animals injected with vehicle (PBS) or HAdV-56-Luc ($P<0.05$) (Fig. 5d), and in comparison to non-depleted HAdV-5-injected animals. There were no significant differences in ALT levels amongst any of the groups. Serum aminotransferase elevation was not observed in any of the HAdV-56-Luc-inoculated animals, indicating reduced liver toxicity compared with HAdV-5 vectors.

HAdV-56 induces an inflammatory immune response

Previous reports have demonstrated a potent inflammatory immune response against Ad vectors in the hours following i.v. administration. We investigated the levels of cytokines and chemokines induced following i.v. delivery of PBS, HAdV-56-Luc or HAdV-5-Luc by harvesting mouse serum samples at 6 h post-i.v. administration of vectors and testing the sera against a mouse multiplex panel. In the absence of clodronate liposome treatment (CL−) HAdV-56-Luc induced higher levels of pro-inflammatory mediators than were observed in macrophage-depleted mice (CL+), and in general these were elevated above the levels observed in HAdV-5-Luc- or PBS-inoculated animals (Fig. 6). The IFNγ and tumour necrosis factor α (TNFα) levels were higher in CL− animals treated with HAdV-56-Luc compared to those treated with HAdV-5. The levels of cytokines interleukin-5 (IL5) and IL6, and those of chemokines IP10, MCP1 and MIG1, were significantly higher in HAdV-56-injected animals in comparison to those for HAdV-5- or PBS-administered controls. Such differences between the vectors were not as marked in CL+ animals, and in fact the retrieved IL6 was slightly higher in HAdV-5 mice compared to those receiving HAdV-56. Conversely, with the exception of IL6, the responses in HAdV-5 treated mice were largely unaffected by the depletion of macrophages. Taken together, these data indicate that rHAdV-56 triggers a

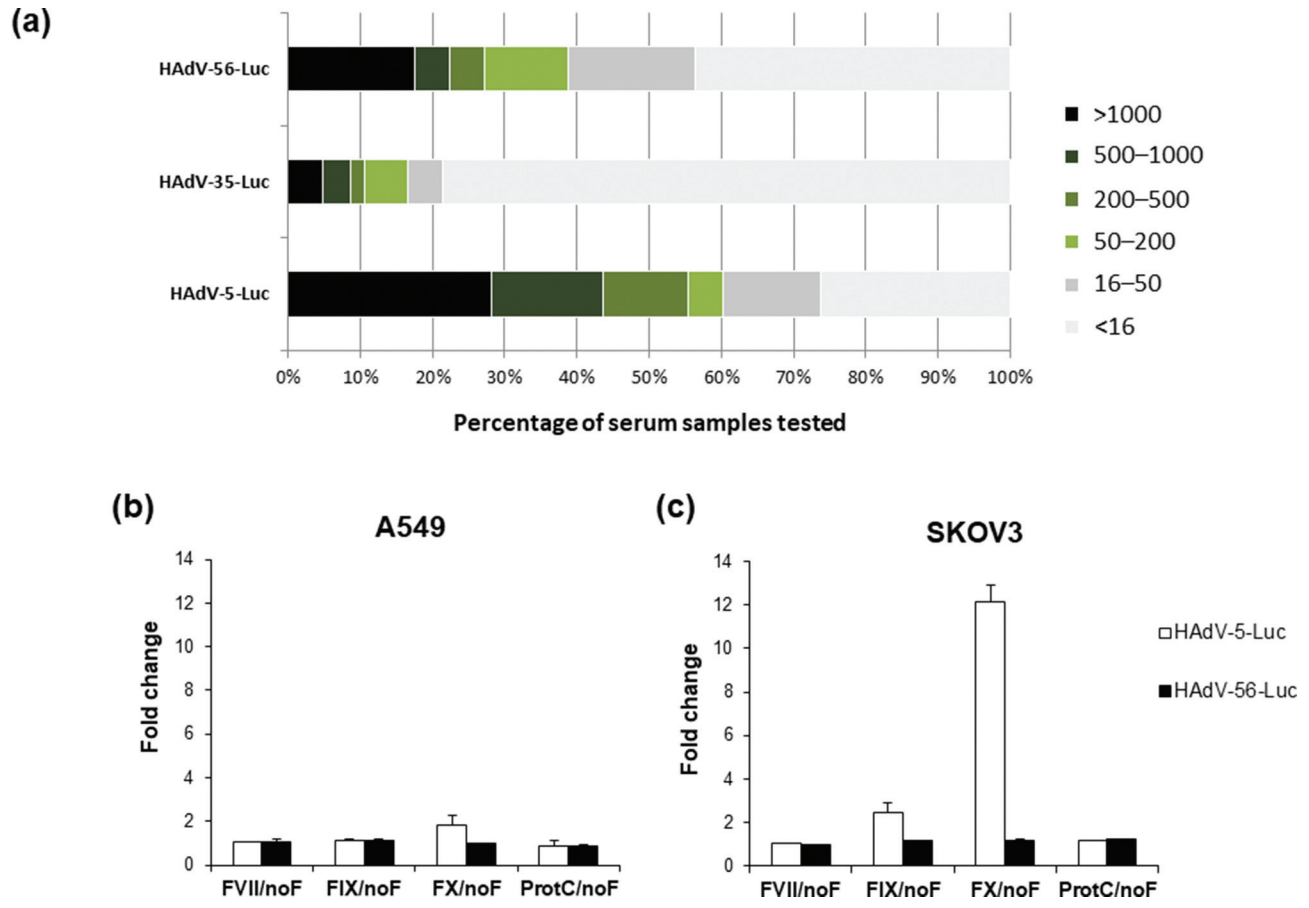

Fig. 4. HAdV-56 interaction with blood components. (a) HAdV-56, HAdV-35 and HAdV-5 seroneutralization by a cohort of healthy >50-year-old US citizens (n=103 individual serum samples). Chart categorizing percentage of sera by neutralization titre. Neutralizing antibody titres were arbitrarily divided into the categories <16 (negative), 16–50, 50–200, 200–500, 500–1000 and >1000 dilutions. (b, c) HAdV-56-Luc transduction assay on (b) A549 and (c) SKOV3 cells in comparison to HAdV-5-Luc. Both were pre-incubated with blood coagulation factors [factor VII (FVII), factor IX (FIX), factor X (FX) and protein C] before being added to cells. Statistical analysis was performed by t-test with Welch's correction: *P< 0.05, **P<0.0002 and ***P<0.0005.

robust inflammatory and cellular immune response *in vivo* following i.v. delivery.

HAdV-56 as a candidate vaccine vector

We next investigated the potential of HAdV-56 as a vaccine vector candidate by performing prime immunizations in Balb/c mice. Species D HAdV-26, a leading vaccine vector that has recently been undergoing clinical trials for HIV and Ebola [37, 38], was used for direct comparison in this study. Mice were immunized intramuscularly with 1×10^{9} VP or 1×10^{10} VP of E1- and E3-deleted HAdV-26 vector expressing luciferase (HAdV-26-Luc) or HAdV-56-Luc. Two weeks post prime immunization, the mice were sacrificed and the serum titres against the HAdV-56 or HAdV-26 based vectors were determined. The induction of Luc-specific IFNγ-producing cells was measured by IFNγ ELISPOT after the splenocytes were stimulated with a 15-mer peptide pool spanning the luciferase protein. HAdV-56-Luc led to the activation of luciferase-specific IFNγ-producing cells, and importantly this was to the same extent as that caused by HAdV-26-Luc immunization (Fig. 7a). An antibody response to the antigen could not be detected for either vector (data not shown). In contrast, there were neutralizing antibodies against HAdV-56-Luc present in the serum of the treated mice (Fig. 7b). This neutralizing activity was similar for HAdV-26 in serum from HAdV-26-Luc animals. Taken together, these data indicate that HAdV-56-Luc induces luciferase-specific IFNγ-producing cells and anti-HAdV-56 neutralizing antibodies in Balb/c mice. Importantly, these effects are observed to the same extent as for HAdV-26, the most clinically advanced human Ad vaccine vector candidate.

DISCUSSION

To advance the use of Ads as therapeutic vectors it is crucial to expand the repertoire of those available by studying rarer types and creating efficient vector platforms. We present the

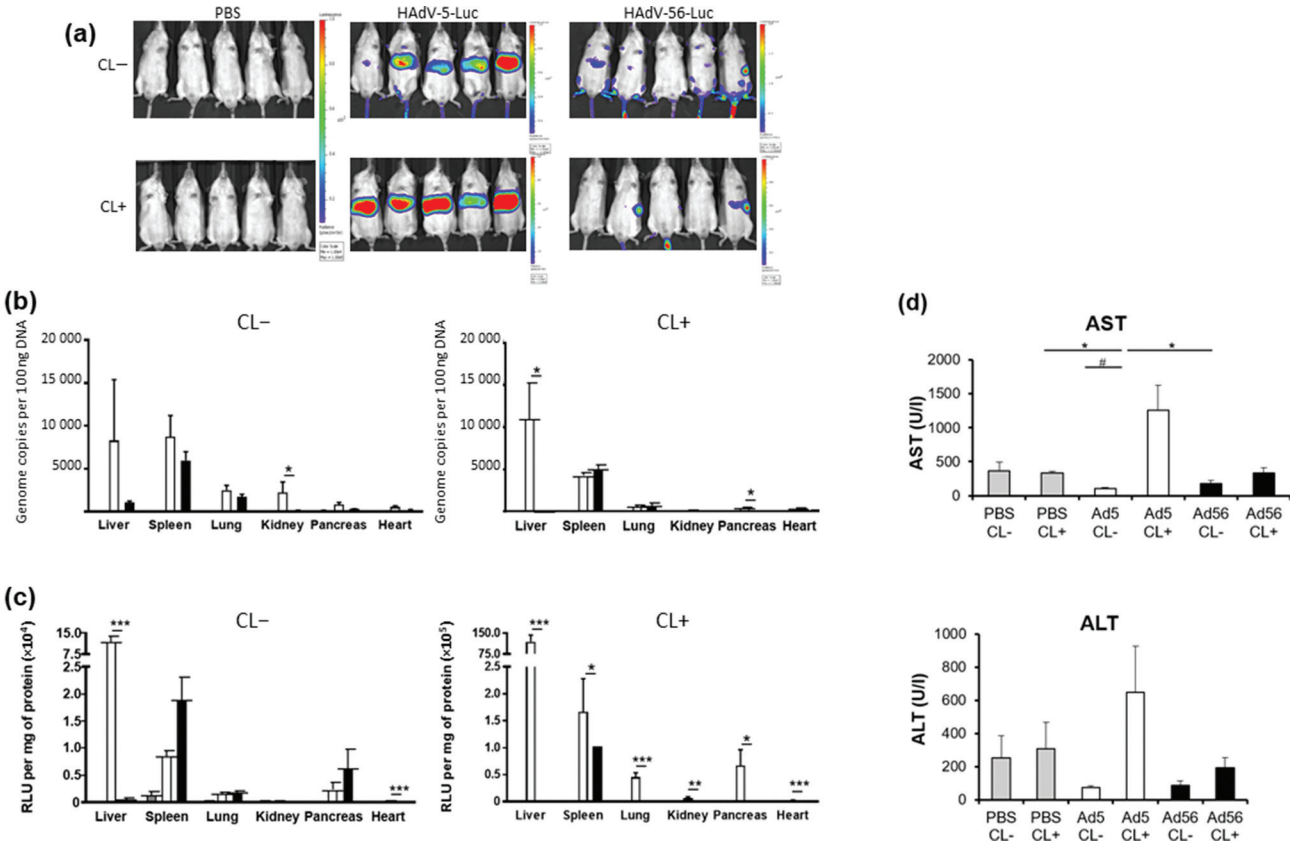

Fig. 5. HAdV-56 biodistribution *in vivo*. HAdV-56-Luc *in vivo* characterization in mice pre-treated or non-treated with clodronate liposomes (CL+, CL−) to avoid macrophage capture of vectors. (a) Representative IVIS for viral biodistribution; (b) Ad genome units per tissue; (c) vector transgene protein activity (luciferase) per tissue. (d) Liver damage state. Statistical comparison between groups was made with a one-tailed *t*-test: #P<0.05 between HAdV-5 groups; *P<0.05 versus PBS and HAdV-56 CL+ groups, respectively.

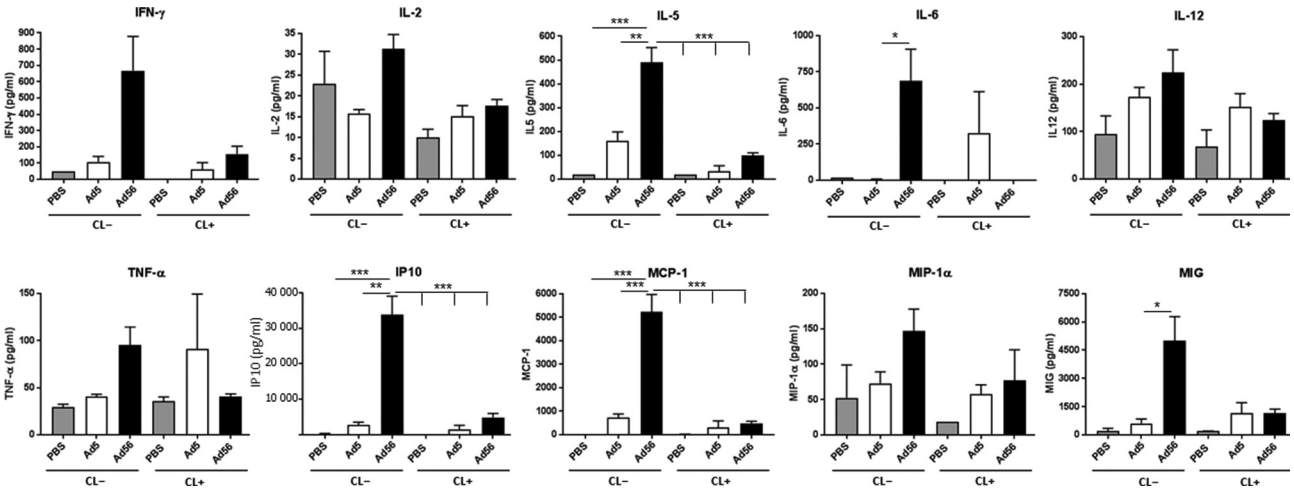

Fig. 6. Cytokine profiles upon i.v. delivery of vectors. Cytokines were measured in blood samples from mice at 6 h following the administration of PBS, HAdV-5-Luc and HAdV-56-Luc. Statistical analysis was performed using one-way ANOVA with Bonferroni's multiple comparison test (IL-5, IP10, MCP-1), or by *t*-test comparison with Welch's correction between not-treated-with-clodronate-liposomes (CL−) HAdV-5 and HAdV-56 groups (IL-6 and MIG). In all cases: *P<0.05, **P<0.01 and ***P<0.005. No statistically significant differences were observed in the others.

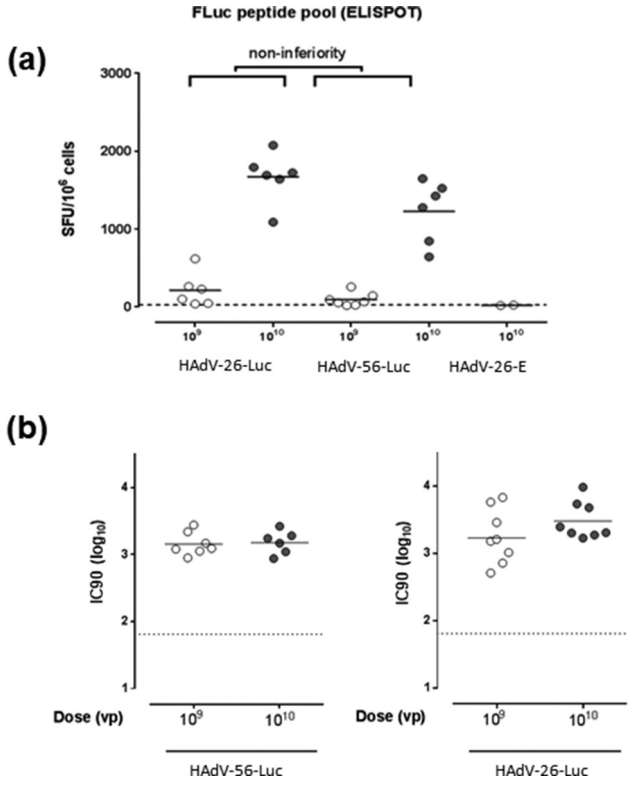

Fig. 7. Prime immunization with HAdV-56 in mice. Mice (n=6–7/group) were immunized intramusculary with HAdV-26-empty (E, no transgene), HAdV-26 or HAdV-56 vectors (1×10^9 VP or 1×10^{10} VP) expressing luciferase protein (Luc). (a) Two weeks post-prime immunization, the mice were sacrificed and the induction of Luc-specific IFNγ-producing cells was measured by IFNγ ELISPOT; splenocytes were stimulated with 15-mer peptide pool-spanning luciferase protein (Luc pool). Each dot represents a mouse, the bar indicates the geometric mean and the dotted line is the 95th percentile based on the medium control samples. (b) The induction of anti-HAdV-56 or anti-HAdV-26 neutralizing antibodies was measured using a standard virus neutralization assay. The dotted line corresponds to the titre of serum from non-vaccinated animals [$\log_{10}(64)$=1.81]. SFU, spot-forming units. Non-inferiority statistical analysis was performed across dose, with HAd26.Luc as the reference group and a pre-specified margin of 0.5 $\log_{10}$.

first report on the generation of ease-of-use cloning systems for HAdV-56 vectors and the initial characterization of *in vitro* and *in vivo* profiles of the recombinant HAdV-56 reporter viruses.

Here, we created a flexible three-plasmid system for HAdV-56 vector generation, allowing for the convenient insertion of transgenes into a multiple cloning site substituting the E1 region. The wild-type (WT) HAdV-56 E4ORF6 region was replaced with that of HAdV-5, a technique that was previously adopted for the generation of HAdV-26, HAdV-48 and HAdV-49 vectors, and enabled their successful production in HAdV-5 E1-complementing cells [13, 15]. Interestingly, we found that both HAdV-56 with the native ORF6 sequence and the HAdV-5 swap could be propagated on HEK293 cells. However, for the vector with the native ORF6 transgene region, instability was observed for large transgene insertions (in 1/10 plaques a truncated transgene region was observed, as indicated by a smaller than expected PCR product), with this being indicative of possible growth problems for this vector (data not shown). HAdV-56-HAdV-5-E4ORF6 allowed for high-quality manufacture at high titres, making large-scale clinical manufacture a viable option.

The efficacy of the frequently used HAdV-5 vector is hampered in clinics by a combination of factors; anti-HAdV-5 immunity, its limited receptor usage, with cellular entry highly dependent on CAR expression *in vitro*, binding to blood factors directing liver tropism and related hepatotoxicity *in vivo*. We found that HAdV-56 did not rely on CAR for *in vitro* cell transduction at the level of HAdV-5, and similarly to that reported for HAdV-26 and HAdV-48, it was not affected by blood coagulation factors [31]. Previous studies have demonstrated that HAdV-Ds can employ subunits of sialic acids and αv integrins as entry receptors/co-receptors [39]. The surprising observation from the neuraminidase-mediated knockdown experiment that sialic acids are not required for HAdV-56 infection of corneal cells suggests that sialic acid-containing GD1a is not a main receptor for HAdV-56, and instead this vector may possess a unique/unusual primary receptor usage and entry pathway. By screening a panel of integrin-expressing cells, we identified a new candidate Ad entry receptor or co-receptor and showed that HAdV-56 probably uses integrin-α7 for cellular transduction *in vitro*. The observation that integrin-α7 may be used as an entry receptor or co-receptor for Ad is a new one, with previous work having mostly defined roles for αv-containing integrins [39]. Whilst we cannot exclude the possibility that other integrins and/or other molecules are also used as receptors/co-receptors by HAdV-56, it is suggestive that HAdV-56 may have a somewhat unique infection profile (Arnberg *et al.*, manuscript in preparation). More recently, a study demonstrated that HAdV-37, another EKC inducer, uses αVβ1 and α3β1 integrins for the infection of human corneal epithelial cells [40]. In this same piece of work, the expression of α2, α3, α6, αV, β1 and β4 integrin subunits in the human corneal epithelium was described, with significantly reduced or no expression of α4, α5, β3, or β5 integrins [40]. The expression of integrins α7–9 was not investigated previously, but given our new findings regarding HAdV-56 infection via α7, the expression of this receptor on human corneal cells may also be highly informative in the context on EKC.

The seroprevalence rate of HAdV-56 was lower than that reported for HAdV-5 and *in vivo* liver targeting and hepatoxicity were absent, which are all beneficial factors for i.v. delivery of vascular gene therapy vectors. It is worth noting that the cohort of healthy volunteers used for the seroprevalence study were all 50+ years old, and this may have led to slightly above average levels of neutralizing antibodies against all vectors. Whilst HAdV-56 showed comparable

levels of transduction in human vascular smooth muscle and endothelial cells to HAdV-5, other Ad-Ds such as HAdV-49, may be better suited to act as a cardiovascular gene therapy for coronary interventions or bypass grafting applications [41, 42]. This is mainly due to the fact that upon *ex vivo* exposure to whole blood, HAdV-56 resulted in the haemagglutination of both human and mouse blood cells (Fig. S4), which raises questions over its suitability for applications where this route of administration is necessary. However, as our data suggest, HAdV-56 may have more leverage as a vaccination vector. The induction of the potent adaptive immunity required for successful vaccination vectors is dependent on sufficient activation of the innate immune system. Vaccine vectors benefit from complement activation and the production and release of cytokines and chemokines, including IL6, TNFα, IFNγ, MCP1, IP10 and MIP1, which are major players in the induction of anti-viral immune responses. HAdV-56 induced higher levels of all the aforementioned mediators, and it was significantly more immunogenic than HAdV-5 following i.v. administration *in vivo*. Whilst these factors may translate to Ad-associated toxicity, making it unsuitable for intravascular delivery, it is worth investigating its use as an intramuscularly delivered vector. In the vaccine vector prime immunization assays used in this study, HAdV-56 achieved the same levels of immune induction as HAdV-26, with similar levels of luciferase-specific IFNγ-producing cells and similar production of anti-Ad immunity. Clinical vaccines based on non-human [43, 44] and human Ads are undergoing extensive development, with exciting results being observed in studies testing HAdV-26 against Ebola and HIV [37, 38, 45, 46]. In preclinical tests, HAdV-26 used alone was demonstrated to induce robust humoral and cellular immunity, while it has also been well tolerated in humans while eliciting target specific immunity in phase I trials. Although it is beyond the scope of this study, it would be interesting to investigate HAdV-56 in a prime boost setting with HAdV-26 to see if this could be successfully incorporated into such regimes. Similar heterologous prime-boost strategies have demonstrated increased potency and greater vaccine efficacy in comparison to homologous prime boost approaches in a range of clinical settings.

To summarize, in this study we have broadened the range of available Ad vector types and have highlighted some of the potential areas in which HAdV-56 could be of therapeutic benefit.

METHODS

Cell lines

HEK293 (human embryonic kidney cells: ATCC CRL-1573) were grown in Dulbecco's modified Eagle's medium (DMEM) supplemented with 10 % foetal bovine serum (FBS; Gibco, UK). A549 (human lung epithelial carcinoma: ATCC CCL-185) and SKOV3 (human ovarian adenocarcinoma: ATCC HTB-77) cells were grown in RPMI-1640, supplemented with 10 % FBS, 1 % penicillin/streptomycin (P/S), 1 % L-glutamine (Gibco) and 1 % Na-Pyr (Sigma, UK). Chinese hamster ovary (CHO) cells, CHO-CAR, CHO-B2, CHO-alpha v, CHO-alpha 4 beta7, CHO-alpha 4 beta1 and CHO-alpha 5 were maintained in DMEM containing 10 % FBS, L-glutamine, nonessential amino acids and G418. CHO-K1, CHO-alpha 2 beta1, CHO-alpha 3, CHO-alpha 6, CHO-alpha 7, CHO-alpha 8 and CHO-alpha 9 were grown in Ham's F-12 medium (Invitrogen, Carlsbad, CA, USA) containing 10 % FBS, HEPES and 1 % P/S.

Construction of replication-deficient recombinant HAdV-56 vectors

The wild-type (WT) HAdV-56 virus, purchased from ATCC, was propagated on HEK293 cells and purified by caesium chloride (CsCl) density gradient centrifugation. The 35 066 bp DNA sequence of WT HAdV-56 is available on GenBank under accession no. HM770721.2.

HAdV-56 cloning system

The HAdV-56 vector construction strategy was based on a three-plasmid system, with sufficient homology between each of the plasmids to enable homologous recombination *in vitro* following the co-transfection in HAdV-5 E1-complementing HEK293 cells. Firstly, adapter plasmids (pAdApt56.ΔE1) containing the left end of the HAdV-56 genome with E1 deletions, and incorporating either luciferase (pAdApt56.ΔE1.Luc), GFP (pAdApt56.ΔE1.GFP) or LacZ (pAdApt56.ΔE1.LacZ) reporter genes, were generated. Briefly, the plasmid pAdApt56.ΔE1 (nt 1–476 of WT HAdV-56) contained the left inverted terminal repeat (ITR) and included an expression cassette consisting of a CMV promoter followed by a multiple cloning site, encompassing Luc, GFP or LacZ within HindIII and XbaI sites, and the SV40 poly(A) signal. This plasmid also contained WT HAdV-56 nt 3369–5917 to allow homologous recombination in HEK293 cells, with the HAdV-56 pBr-based plasmid (pBr.HAdV-56.pIX.Hx) carrying the HAdV-56 genome from pIX to the hexon (nt 3755–19 308). The third plasmid (pBr.HAdV-56.ΔE3.ORF6.rITR) contained the HAdV-56 genome from pVI to the right ITR (nt 17 333–35 066) and had a 4 kb deletion in the E3 region, while the HAdV-5 E4-ORF6 replaced the HAdV-56 E4-ORF6. The HAdV-56 E4-ORF6 was exchanged by the HAdV-5 E4-ORF6 to enable growth of the recombinant HAdV-56 vector on E1 complementing cells as described previously [15]. Deletion of the HAdV-56 E3 region and swapping of the HAdV-56 E4-ORF6 for that of HAdV-5 was performed using the Gibson assembly methodology [47]. Briefly, pBr.HAdV-56.ΔE3.ORF6.rITR was constructed by generating two PCR fragments flanking the HAdV-56 E3 region (nt 17 333–26 625 and 30 622–32 015) using primers to artificially introduce complementary overhangs and allow the ligation of both PCR fragments, thereby deleting ~4 kb of the HAdV-56 E3 region (nt 26 626–30 621). The HAdV-56 E4-ORF6 sequence from nt 32 016 to 33 221 was replaced by the corresponding sequence of HAdV-5 by generating two additional PCR fragments, one with the HAdV-5 E4-ORF6 (HAdV-5 GenBank accession no. M73260 nt 32 963–

34 077) and another with the right arm of HAdV-56 (nt 33 222–35 066), again with artificially introduced complementary overhangs. Q5 high-fidelity DNA polymerase (NEB) was used for all PCR reactions. The PCR fragments (1 pmol total DNA) were incubated together at 50 °C for 1 h in the presence of 10 µl Gibson assembly master mix (NEB), and this was followed by transformation in 10-beta competent *E. coli* (NEB).

HAdV-56 plasmid transfection, amplification and titre quantification

Reconstitution of the full-length recombinant HAdV-56 vector (rHAdV-56.ΔE1.ΔE3.5ORF6 or rHAdV-56 for short) expressing luciferase, GFP or β-galactosidase (LacZ) was accomplished by homologous recombination via co-transfection of pAdApt56.ΔE1.Luc/GFP/LacZ, pBr.HAdV-56.pIX.Hx and pBr.HAdV-56.ΔE3.ORF6.rITR in HEK293 cells using Lipofectamine 2000 (Invitrogen). Following cytopathogenic effect, HAdV-56 vectors were harvested and further propagated on HEK293 cells. Purified HAdV-56 vectors were obtained by two-step CsCl gradient centrifugation [48]. Whole viral genomes were fully sequenced at Glasgow Polyomics by NGS with Illumina adapters. Viruses were also verified by silver stain analysis and Western blot using the anti-fibre 4D2 antibody (1 : 500 dilution). Virus particle titres were determined by OD260 measurement in the presence of SDS. Viral infectious units were determined by $TCID_{50}$ analysis. The VP:PFU ratios were in the range of 1 : 200–285 for all vectors. In all of the experiments the HAdV-56 performance was compared to that of Ad vectors that expressed the same recombinant reporter gene under the control of the same regulatory sequences.

HAdV-56 vector manufacture

HEK293 suspension cells were seeded at a cell density of 1.5×10^6 cells ml^{-1} in 125 ml shaker flasks in a total volume of 15 ml EX-CELL 293, AEM, CD293, CDM4-HEK293, SFM4-HEK293 or EX-CELL GTM-3 medium. The cells were subsequently infected with HAdV-56 (270 VP/cell) and incubated at 110 rpm, 8 % CO_2, 37°C. The harvest was performed at day 3 post-infection (p.i.) and the infectious virus yield was determined by $TCID_{50}$ analysis.

To investigate different purification methods, CsCl purified virus was first spiked in spent medium of HEK293 cells to determine the retention time of the virus peak after purification using Mustang Q, Poros HQ or Monolith QA chromatography. The virus yield after this purification step was determined by $TCID_{50}$. To obtain a scalable process, HEK293 suspension cells were seeded at a cell density of 1.5×10^6 cells ml^{-1} in shaker flasks using EX-CELL 293 medium, and infected with HAdV-56 (270 VP cell^{-1}). At day 3 p.i., a crude harvest was obtained, treated with benzonase and subsequently purified using the same linear gradients as the initial spike experiments to confirm the previous findings. The fraction containing the viral peak was determined and subsequently step gradients were performed on all AIEX purifications using a step after loading for the elution of contaminants and a step with a higher salt concentration for the elution of the viral peak. The obtained materials were tested for purity using SDS-PAGE.

Viral transduction assays

The cells were seeded at 1×10^4 cells well^{-1}. The following day monolayers were washed with PBS and viral vectors were added at the indicated VP/cell concentrations in their corresponding media without serum. After 3 h at 37 °C, the medium was replaced with 200 µl well^{-1} of medium supplemented with 10 % FBS, and the cells were incubated for a further 48 h. In the experiments in which blood coagulation factors were used, these were pre-incubated with the vectors for 30 min at 37 °C before they were added to the cells. The blood coagulation factors were purchased from Cambridge Bioscience and used at physiological concentrations: FVII at 0.5 µg ml^{-1}, FIX at 5 µg ml^{-1}, FX at 10 µg ml^{-1} and protein C at 4.5 µg ml^{-1}. For the assay readout, the plates were washed and the cells lysed with 1× reporter lysis buffer (100 µl per well; Promega) and one freeze-thaw cycle was performed. Luciferase (Luciferase assay system, Promega) and BCA protein quantitation assays (ThermoFisher Scientific) were performed with 10 µl of lysed cells in white opaque plates (Greiner BioOne) following the manufacturer's instructions and the results were recorded in a Victor X multilabel plate reader (Perkin-Elmer). Luciferase activity was normalized to the total protein content of the sample wells and transduction was calculated as a percentage of the control. The transduction level was expressed as luminescence relative light units per mg of protein per well (RLU mg^{-1}). All of the assays were performed in triplicate.

Sialic acid receptor studies

HAdV-56 binding

Metabolically ^{35}S-labelled HAdV-56 virions were produced in A549 cells as described previously [49], with some minor modifications, i.e. the elution was performed in phosphate-buffered saline (PBS) using a NAP column (GE Healthcare). Human corneal epithelial (HCE) cells were grown in SHEM media [SHEM media: 1 : 1; DMEM and Ham's F12 nutrient mixture supplemented with 20 mM HEPES, 5 µg ml^{-1} insulin, 0.5 % DMSO, 0.1 µg ml^{-1} cholera toxin, 10 ng ml^{-1} hEGF, PEST (20 U ml^{-1} penicillin + 20 g ml^{-1} streptomycin) and 10 % FCS]. The cells were detached with pre-warmed PBS containing 0.05 % EDTA, reactivated in growth medium for 1 h at 37 °C (in suspension). The cells were then pelleted in a V-bottom 96-well plate (1×10^5 cells well^{-1}) and washed once with binding buffer (BB) [BB: DMEM supplemented with 20 mM HEPES, PEST and 1 % bovine serum albumin (BSA)]. The cells were treated with or without neuraminidase (20 mU ml^{-1}, *Vibrio cholerae* neuraminidase; Sigma) for 1 h at 37 °C before being incubated with virions. The cells were washed twice with BB to remove the neuraminidase. Metabolically ^{35}S-labelled HAdV-56 virions (10^9VP well^{-1}) diluted in BB were added to the cells and incubated for 1 h at 4 °C on ice. To get rid of unbound virions, the cells were washed twice with PBS.

Cell-associated radioactivity was measured using a Wallac 1409 liquid scintillation counter (Perkin-Elmer).

HAdV-56 infection

HCE cells were grown as a monolayer in a transparent flat-bottom 96-well plate (3 0 000 cells well^{-1}). The cells were then washed twice with serum-free growth medium (SFGM). The cells were treated with or without neuraminidase (20 mU ml^{-1}) for 1 h at 37 °C. The cells were washed twice with SFGM to remove the neuraminidase. WT HAdV-56 virions were added to the cells and incubated for 1 h on ice. To get rid of unbound virions the cells were washed thrice with SFGM. The cells were incubated for 44 h at 37 °C in culture medium containing 1 % FBS. After 44 h incubation, the cells were washed once with PBS (pH 7.4) and fixed with ice-cold methanol at −20 °C. The cells were then stained with mouse monoclonal anti-HAdV hexon antibody diluted in PBS (1 : 200) for 1 h at room temperature (RT). The cells were washed thrice with PBS and incubated for 1 h with Alexa Fluor-488-conjugated secondary antibody (1 : 1000) diluted in PBS at RT. The cells were also stained with DAPI (1 : 5000) diluted in PBS for another 5 min. After the cells were washed thrice with PBS, the number of infected cells was counted in Trophos (Luminy Biotech Enterprises).

Integrin co-receptor usage assays

The cells (CHO, CHO-B2, CHO-alpha v, CHO-alpha 4 beta7, CHO-alpha 4 beta1, CHO-alpha 5, CHO-K1, CHO-alpha 2 beta1, CHO-alpha 3, CHO-alpha 6, CHO-alpha 7, CHO-alpha 8 and CHO-alpha 9) were plated in duplicate wells in 96-well tissue culture plates and transduced with HAdV-5-GFP (3.7×10^4 VP cell^{-1}) and HAdV-56-GFP (1.2×10^4 VP cell^{-1}). The cultures were maintained at 37 °C in a humidified atmosphere with 5 % CO_2. At 24 h after infection, automated fluorescent image acquisition was performed for each individual well of a 96-well plate using Trophos Plate RUNNER HD (Trophos, Marseille, France). The images acquired from the wells were analysed using Tina software (Trophos).

HAdV-56 seroneutralization

Serological inhibition of HAdV-56-Luc, HAdV-35-Luc and HAdV-5-Luc transduction was evaluated over a collection of 103 serum samples from a cohort of healthy >50-year-old US citizens. Seroneutralization assays were performed using the protocol described in Sprangers *et al.* [50]. Briefly, serum samples were heat-inactivated at 56 °C for 60 min, and then twofold dilutions were performed in a 96-well tissue culture plate. The dilutions covered a range from 1/16 to 1/4 096 in an end volume of 50 µl DMEM. Negative controls consisted of DMEM alone. We added 50 µl of virus solution (1×10^8 VP ml^{-1}) to each well. Next, a cell suspension (10^4 A549 cells) was added to the well to a final volume of 200 ul. Following 24 h incubation, the luciferase activity in the cells was measured using a Steady-Glo luciferase reagent system (Promega). The neutralization titres were defined as the maximum serum dilution that neutralized 90 % of luciferase activity.

In vivo biodistribution

All animal experimentation was approved by the University of Glasgow Animal Procedures and Ethics committee and was performed under UK Home Office license in strict accordance with UK Home Office guidelines. Male outbred MF1 immunocompetent mice aged between 7–9 weeks (Harlan, Blackthorn, UK) were used. The animals were organized in six groups with five animals in each group. To deplete macrophages, 200 µl of clodronate-encapsulated liposomes (www.clodronateliposomes.org) was administered i.v. to half of the groups 48 h before the administration of the vectors. Intravenous injections were performed via the tail lateral vein. On day 0, treatment groups were i.v. injected with 5×10^{10} VP of HAdV-56-Luc or HAdV-5-Luc diluted in 100 µl PBS. Matched control groups were injected with 100 µl PBS at the same time-point. Blood was taken at 6 h post-vector delivery and the serum was separated as previously described [30]. Cytokine/chemokine profiles were determined from 6 h post-injection sera (>60 µl) using a mouse cytokine multiplex assay kit (Invitrogen) and a Luminex machine (Luminex Corporation). At 48 h post-delivery of vectors, the animals were sacrificed and their livers, spleens, lungs, kidney, pancreases and hearts collected for the quantification of viral genomes by the amplification of the transgene region promoter with CMV primers and the measurement of luciferase activity as described previously [51]. Blood was also collected at the end point, and the serum was segregated (80 µl) and used for the quantification of the transaminases ALT and AST as previously described [35].

Mouse immunization study

All animal experimentation was performed according to Dutch law and the Guidelines on the Protection of Experimental Animals published by the Council of the European Committee. Six-to-eight-week-old specific pathogen-free female Balb/c mice were purchased from Charles River and kept at the institutional animal facility under specified pathogen-free conditions. For prime immunization studies mice were immunized intramuscularly with HAdV-56 or HAdV-26 vectors (1×10^9 VP or 1×10^{10} VP mouse^{-1}) expressing Luc. Two weeks post-immunization, mice were sacrificed and the induction of Luc-specific IFNγ-producing cells was measured by IFNγ ELISPOT. In brief, mouse splenocytes were stimulated with 15-mer peptide pool spanning Luc (luc pool), medium (control negative) or phorbol myristate acetate (PMA; positive control). For the presentation of data each dot on the graph represents a mouse, the bar indicates the geometric mean and the dotted line is the 95th percentile based on the medium control samples. The induction of anti-HAdV-56 neutralizing antibodies was measured using a standard virus neutralization assay as mentioned above, but the dilutions tested ranged from 1/64 down to 1/16 384 [50]. The dotted line on the graph corresponds to the $\log_{10}$ of the highest serum concentration used [$\log_{10}(64)$=1.81].

Statistical analysis

Statistical analysis was performed with GraphPad Prism software. One-way ANOVA with the Bonferroni post-hoc test was used for comparisons between more than two groups, whereas statistical comparison between two groups was made using a *t*-test. The parameters of significance are indicated in each figure caption: $*P<0.05$, $**P<0.005$, $***P<0.001$ and NS, not statistically significant, $P>0.05$. The presented *in vitro* results are averaged data from at least three different experiments with three experimental replicates per condition. The *in vivo* experiments were performed with a minimum of five animals per group. All of the errors bars represent the standard error of the mean (SEM). For Fig. 7a statistical analyses were performed with SAS version 9.4. Non-inferiority testing across dose was performed on $\log_{10}$-transformed data, with HAdV-26-Luc as a reference and a pre-specified margin of 0.5 log.

Funding information
Most of the authors are funded by the Framework 7 Industry Academy Partnership Programme AD-VEC (agreement number 324325). One author was funded by the Framework 7 Programme ADVANCE (agreement number 290002). The funders had no role in study design, data collection and interpretation, or the decision to submit the work for publication.

Acknowledgements
We would like to thank Nicola Britton, Elaine Friel, Gregor Aitchison and Ryan Ritchie for their excellent technical support at the Institute of Cardiovascular and Medical Sciences (ICAMs), Glasgow, UK.

Conflicts of interest
J. C. and S. K are employees of Janssen Vaccines and Prevention BV, The Netherlands. M. B, E. H, A. L and M. H. are employees of Batavia Bioservices, The Netherlands.

Ethical statement
The ethical committee of the University of Glasgow approved the use of human samples for this study, and all subjects involved provided informed consent. All work involving animals was approved by the University of Glasgow Animal Procedures and Ethics committee and was performed under UK Home Office license in strict accordance with UK Home Office guidelines. Furthermore, the animal work shown in Fig. 7, was performed according to the Dutch law and the Guidelines on the Protection of Experimental Animals published by the Council of the European Committee (EU directive 86/609) after approval by the Dier Experimenten Commissie of Crucell (permit number 21300).

References

1. Sasaki T, Tazawa H, Hasei J, Osaki S, Kunisada T *et al.* A simple detection system for adenovirus receptor expression using a telomerase-specific replication-competent adenovirus. *Gene Ther* 2013;20:112–118.
2. Zhang W, Fu J, Liu J, Wang H, Schiwon M *et al.* An engineered virus library as a resource for the spectrum-wide exploration of virus and vector diversity. *Cell Rep* 2017;19:1698–1709.
3. Belousova N, Mikheeva G, Xiong C, Stagg LJ, Gagea M *et al.* Native and engineered tropism of vectors derived from a rare species D adenovirus serotype 43. *Oncotarget* 2016;7:53414–53429.
4. Weaver EA, Barry MA. Low seroprevalent species D adenovirus vectors as influenza vaccines. *PLoS One* 2013;8:e73313.
5. Kahl CA, Bonnell J, Hiriyanna S, Fultz M, Nyberg-Hoffman C *et al.* Potent immune responses and *in vitro* pro-inflammatory cytokine suppression by a novel adenovirus vaccine vector based on rare human serotype 28. *Vaccine* 2010;28:5691–5702.
6. Ruzsics Z, Wagner M, Osterlehner A, Cook J, Koszinowski U *et al.* Transposon-assisted cloning and traceless mutagenesis of adenoviruses: development of a novel vector based on species D. *J Virol* 2006;80:8100–8113.
7. Alonso-Padilla J, Papp T, Kaján GL, Benkő M, Havenga M *et al.* Development of novel adenoviral vectors to overcome challenges observed with HAdV-5-based constructs. *Mol Ther* 2016;24:6–16.
8. Chen H, Xiang ZQ, Li Y, Kurupati RK, Jia B *et al.* Adenovirus-based vaccines: comparison of vectors from three species of adenoviridae. *J Virol* 2010;84:10522–10532.
9. Nemerow GR, Stewart PL. Insights into adenovirus uncoating from interactions with integrins and mediators of host immunity. *Viruses* 2016;8:337.
10. Nilsson EC, Storm RJ, Bauer J, Johansson SM, Lookene A *et al.* The GD1a glycan is a cellular receptor for adenoviruses causing epidemic keratoconjunctivitis. *Nat Med* 2011;17:105–109.
11. Arnberg N, Kidd AH, Edlund K, Olfat F, Wadell G. Initial interactions of subgenus D adenoviruses with A549 cellular receptors: sialic acid versus alpha(v) integrins. *J Virol* 2000;74:7691–7693.
12. Burmeister WP, Guilligay D, Cusack S, Wadell G, Arnberg N. Crystal structure of species D adenovirus fiber knobs and their sialic acid binding sites. *J Virol* 2004;78:7727–7736.
13. Abbink P, Lemckert AA, Ewald BA, Lynch DM, Denholtz M *et al.* Comparative seroprevalence and immunogenicity of six rare serotype recombinant adenovirus vaccine vectors from subgroups B and D. *J Virol* 2007;81:4654–4663.
14. Robinson CM, Singh G, Henquell C, Walsh MP, Peigue-Lafeuille H *et al.* Computational analysis and identification of an emergent human adenovirus pathogen implicated in a respiratory fatality. *Virology* 2011;409:141–147.
15. Havenga M, Vogels R, Zuijdgeest D, Radosevic K, Mueller S *et al.* Novel replication-incompetent adenoviral B-group vectors: high vector stability and yield in PER.C6 cells. *J Gen Virol* 2006;87:2135–2143.
16. Nevels M, Spruss T, Wolf H, Dobner T. The adenovirus E4orf6 protein contributes to malignant transformation by antagonizing E1A-induced accumulation of the tumor suppressor protein p53. *Oncogene* 1999;18:9–17.
17. Enomoto M, Okafuji T, Okafuji T, Chikahira M, Konagaya M *et al.* Isolation of an intertypic recombinant human adenovirus (candidate type 56) from the pharyngeal swab of a patient with pharyngoconjunctival fever. *Jpn J Infect Dis* 2012;65:457–459.
18. Huang G, Yao W, Yu W, Mao L, Sun H *et al.* Outbreak of epidemic keratoconjunctivitis caused by human adenovirus type 56, China, 2012. *PLoS One* 2014;9:e110781.
19. Hiroi S, Furubayashi K, Kawahata T, Morikawa S, Kase T. A case of urethritis caused by human adenovirus type 56. *Jpn J Infect Dis* 2012;65:273–274.
20. Singh G, Zhou X, Lee JY, Yousuf MA, Ramke M *et al.* Recombination of the epsilon determinant and corneal tropism: Human adenovirus species D types 15, 29, 56, and 69. *Virology* 2015;485:452–459.
21. Zhang XP, Puzon-Mclaughlin W, Irie A, Kovach N, Prokopishyn NL *et al.* $\alpha 3\beta 1$ 1 adhesion to laminin-5 and invasin: critical and differential role of integrin residues clustered at the boundary between α 3 N-terminal repeats 2 and 3. *Biochemistry* 1999;38:14424–14431.
22. Eto K, Huet C, Tarui T, Kupriyanov S, Liu HZ *et al.* Functional classification of ADAMs based on a conserved motif for binding to integrin $\alpha 9\beta 1$: implications for sperm-egg binding and other cell interactions. *J Biol Chem* 2002;277:17804–17810.
23. Lu M, Munger JS, Steadele M, Busald C, Tellier M *et al.* Integrin $\alpha 8\beta 1$ mediates adhesion to LAP-TGF$\beta 1$. *Journal of Cell Science* 2002;115:4641–4648.
24. Eto K, Puzon-Mclaughlin W, Sheppard D, Sehara-Fujisawa A, Zhang XP *et al.* RGD-independent binding of integrin $\alpha 9\beta 1$ to the ADAM-12 and -15 disintegrin domains mediates cell-cell interaction. *J Biol Chem* 2000;275:34922–34930.

25. **Mould AP, Askari JA, Humphries MJ.** Molecular basis of ligand recognition by integrin $\alpha 5\beta 1$. I. Specificity of ligand binding is determined by amino acid sequences in the second and third NH2-terminal repeats of the α subunit. *J Biol Chem* 2000;275: 20324–20336.
26. **Isobe T, Hisaoka T, Shimizu A, Okuno M, Aimoto S *et al.*** Propolypeptide of von Willebrand factor is a novel ligand for very late antigen-4 integrin. *J Biol Chem* 1997;272:8447–8453.
27. **Irie A, Kamata T, Puzon-Mclaughlin W, Takada Y.** Critical amino acid residues for ligand binding are clustered in a predicted beta-turn of the third N-terminal repeat in the integrin alpha 4 and alpha 5 subunits. *Embo J* 1995;14:5550–5556.
28. **Schreiner CL, Bauer JS, Danilov YN, Hussein S, Sczekan MM *et al.*** Isolation and characterization of Chinese hamster ovary cell variants deficient in the expression of fibronectin receptor. *J Cell Biol* 1989;109:3157–3167.
29. **Flintoff-Dye NL, Welser J, Rooney J, Scowen P, Tamowski S *et al.*** Role for the $\alpha 7\beta 1$ integrin in vascular development and integrity. *Dev Dyn* 2005;234:11–21.
30. **Yao CC, Breuss J, Pytela R, Kramer RH.** Functional expression of the alpha 7 integrin receptor in differentiated smooth muscle cells. *J Cell Sci* 1997;110:1477–1487.
31. **Waddington SN, Mcvey JH, Bhella D, Parker AL, Barker K *et al.*** Adenovirus serotype 5 hexon mediates liver gene transfer. *Cell* 2008;132:397–409.
32. **Qiu Q, Xu Z, Tian J, Moitra R, Gunti S *et al.*** Impact of natural IgM concentration on gene therapy with adenovirus type 5 vectors. *J Virol* 2015;89:3412–3416.
33. **Shayakhmetov DM, Gaggar A, Ni S, Li ZY, Lieber A.** Adenovirus binding to blood factors results in liver cell infection and hepatotoxicity. *J Virol* 2005;79:7478–7491.
34. **Parker AL, Waddington SN, Nicol CG, Shayakhmetov DM, Buckley SM *et al.*** Multiple vitamin K-dependent coagulation zymogens promote adenovirus-mediated gene delivery to hepatocytes. *Blood* 2006;108:2554–2561.
35. **Coughlan L, Bradshaw AC, Parker AL, Robinson H, White K *et al.*** Ad5:Ad48 hexon hypervariable region substitutions lead to toxicity and increased inflammatory responses following intravenous delivery. *Mol Ther* 2012;20:2268–2281.
36. **Bradshaw AC, Coughlan L, Miller AM, Alba R, van Rooijen N *et al.*** Biodistribution and inflammatory profiles of novel penton and hexon double-mutant serotype 5 adenoviruses. *J Control Release* 2012;164:394–402.
37. **Milligan ID, Gibani MM, Sewell R, Clutterbuck EA, Campbell D *et al.*** Safety and immunogenicity of novel adenovirus type 26- and modified vaccinia ankara-vectored ebola vaccines: a randomized clinical trial. *JAMA* 2016;315:1610–1623.
38. **Baden LR, Karita E, Mutua G, Bekker LG, Gray G *et al.*** Assessment of the safety and immunogenicity of 2 novel vaccine platforms for HIV-1 prevention: a randomized trial. *Ann Intern Med* 2016;164:313–322.
39. **Arnberg N.** Adenovirus receptors: implications for targeting of viral vectors. *Trends Pharmacol Sci* 2012;33:442–448.
40. **Storm RJ, Persson BD, Skalman LN, Frängsmyr L, Lindström M *et al.*** Human adenovirus type 37 uses $\alpha V\beta 1$ and $\alpha 3\beta 1$ integrins for infection of human corneal cells. *J Virol* 2017;91.
41. **Dakin RS, Parker AL, Delles C, Nicklin SA, Baker AH.** Efficient transduction of primary vascular cells by the rare adenovirus serotype 49 vector. *Hum Gene Ther* 2015;26:312–319.
42. **Thirion C, Lochmüller H, Ruzsics Z, Boelhauve M, König C *et al.*** Adenovirus vectors based on human adenovirus type 19a have high potential for human muscle-directed gene therapy. *Hum Gene Ther* 2006;17:193–205.
43. **Ledgerwood JE, DeZure AD, Stanley DA, Coates EE, Novik L *et al.*** Chimpanzee adenovirus vector ebola vaccine. *N Engl J Med* 2017; 376:928–938.
44. **Antrobus RD, Coughlan L, Berthoud TK, Dicks MD, Hill AV *et al.*** Clinical assessment of a novel recombinant simian adenovirus ChAdOx1 as a vectored vaccine expressing conserved Influenza A antigens. *Mol Ther* 2014;22:668–674.
45. **Barouch DH, Picker LJ.** Novel vaccine vectors for HIV-1. *Nat Rev Microbiol* 2014;12:765–771.
46. **Baden LR, Walsh SR, Seaman MS, Tucker RP, Krause KH *et al.*** First-in-human evaluation of the safety and immunogenicity of a recombinant adenovirus serotype 26 HIV-1 Env vaccine (IPCAVD 001). *J Infect Dis* 2013;207:240–247.
47. **Gibson DG, Young L, Chuang RY, Venter JC, Hutchison CA *et al.*** Enzymatic assembly of DNA molecules up to several hundred kilobases. *Nat Methods* 2009;6:343–345.
48. **Nicklin SA, Baker AH.** Simple methods for preparing recombinant adenoviruses for high-efficiency transduction of vascular cells. *Methods Mol Med* 1999;30:271–283.
49. **Johansson SM, Nilsson EC, Elofsson M, Ahlskog N, Kihlberg J *et al.*** Multivalent sialic acid conjugates inhibit adenovirus type 37 from binding to and infecting human corneal epithelial cells. *Antiviral Res* 2007;73:92–100.
50. **Sprangers MC, Lakhai W, Koudstaal W, Verhoeven M, Koel BF *et al.*** Quantifying adenovirus-neutralizing antibodies by luciferase transgene detection: addressing preexisting immunity to vaccine and gene therapy vectors. *J Clin Microbiol* 2003;41:5046–5052.
51. **Ma J, Duffy MR, Deng L, Dakin RS, Uil T *et al.*** Manipulating adenovirus hexon hypervariable loops dictates immune neutralisation and coagulation factor X-dependent cell interaction in vitro and in vivo. *PLoS Pathog* 2015;11:e1004673.